Z. Kristallogr. Proc. **1** (2011) 75-80 / **DOI** 10.1524/zkpr.2011.0011
© by Oldenbourg Wissenschaftsverlag, München

High energy milling of Cu_2O powders

D. Dodoo-Arhin, G. Vettori, M. D'Incau, M. Leoni*, P. Scardi

University of Trento, Department of Material Engineering, Trento, Italy
* Contact author; e-mail: Matteo.Leoni@unitn.it

Keywords: high energy milling, Whole Powder Pattern Modelling

Abstract. Whole Powder Pattern Modelling was employed to investigate the microstructure changes in Cu_2O powders milled in a vibrating cup mill. The reduction in the average size of coherently scattering domains - and simultaneous narrowing of the size distribution - occurs in the first minutes. An asymptotic limit of ca. 10 nm is obtained. The reduction in size is obtained at the expenses of introducing a massive quantity of dislocations in the system, reaching a limit of ca. 4×10^{-16} m^{-2}. A proper nanocrystalline microstructure can be obtained with an effective milling time of ca. 20 min.

Introduction

Nano-sized particles keep attracting the attention of the scientific community because of their peculiar properties arising both from the high surface/volume ratio and from the possible quantum confinement effects. Several methods have been proposed for the synthesis of nanostructured materials. Among them, high energy milling has an undoubted technological importance as it allows producing large quantities of powder in short time and at competitive prices [1]. The microstructure of the nanostructured materials resulting from milling can be conveniently investigated by microscopy and by X-ray diffraction (XRD). XRD of nanocrystalline powders guarantees a better statistical significance of the result, as the information is collected on a much larger quantity of grains (millions versus tens analyzed under the microscope). Line Profile Analysis (LPA) is the group of techniques employed for microstructure analysis from diffraction data, as they are based on the analysis of the broadening of the diffraction peaks [2]. It should be recalled that the broadening of the X-ray diffraction line profiles is determined by instrumental features but also by the small size of the coherently scattering domains (aka crystallites) and by lattice distortions (dislocations, stacking faults, etc). The most widespread techniques for microstructure analysis based on XRD data are certainly the Scherrer formula [3] and the Williamson-Hall plot [4], that are quite often used without care on the underlying theory or hypotheses, and imposing an arbitrary shape to the peaks. The state of the art alternative is offered by full pattern methods, like, e.g., the Whole Powder Pattern Modelling (WPPM) [5], that provides for an interpretation of the whole diffraction pattern in terms of physical models for the broadening sources.
Cuprite Cu_2O is a wide bandgap (2.0–2.2eV) p-type semiconductor that finds important technological applications e.g. in solar cells, gas sensors chemical refinement catalysis and

water splitting [6-9]. The possibility of producing nanostructured Cu_2O could led to an increased activity of the material [10]. We report here the successful reduction in size of a commercial cuprite powder and its microstructural analysis via XRD and microscopy.

Methods

Commercial Cu_2O (99.99+%, Aldrich) was employed as starting material. A high contamination from Cu and CuO was found. The powder was thus subjected to thermal oxidation at 850 °C and 9.5 mbar for 1 h and subsequently stored in sealed containers under Ar atmosphere. The heat treated powder was milled in a Fristch Pulverisette 9 Vibromill (-20°C) using a customised ferritic steel grinding set [11]. A cup of 120ml (nominal volume) and a 662.20 g crushing cylinder were used. Approximately 3.0 g of Cu_2O were milled with 4 %wt ethanol for 1, 5, 7.5, 10, 20 and 40 min, respectively (specimens named P9-1 through P9-40). The given time represents the actual milling time: the process time, however was much longer. In fact, to limit possible effects of heating - leading e.g. to recrystallization - milling was done in batch cycles consisting of a 1 minute milling followed by 5 minutes pause.
X-ray diffraction data were collected on the ID31 high-resolution powder diffraction beamline at the European Synchrotron Radiation Facility (ESRF) in Grenoble - France. The information collected every 15ms from the nine detectors installed on the ID31 goniometer, was suitably mixed and re-binned to provide diffraction patterns in the 2.0° - 65.0° 2θ range with an angular increment of 0.005°. A wavelength of 0.3999284 Å was chosen, calibrated with the NIST SRM 640b Si standard. In order to obtain the best pattern quality (no specimen holder effects), the powder was mounted free standing in a 5x5 mm silicon frame (500 μm thickness) and measured in θ/2θ scanning mode (parallel-beam transmission geometry). The diffraction pattern of the NIST SRM 660a LaB_6 line profile standard was also collected under the same experimental conditions, as to characterize the instrumental effects on the diffraction line profiles. A set of 20 evenly spaced peaks was simultaneously fitted with symmetrical pseudo-Voigt functions whose width and shape was constrained according to the Caglioti *et al.* formulae [12]. The PM2K software [13] was used.
Qualitative phase analysis was done using the PANAlytical X'pert Highscore software and the ICDD PDF-4+ database. Quantification was then obtained via the Rietveld method [14] using the TOPAS software [15].The WPPM method [5] implemented in PM2K [13] was employed for the microstructure analysis.
An FEI XL30 Environmental Scanning Electron Microscope (ESEM) was employed for microscopy analysis. Specimens were metalized and analyzed at 30 kV, 93 μA and 0.7 Torr (water pressure). HRTEM was carried out on a JEOL 2100 URP microscope equipped with a Gatan "Ultrascan" 2k x 2k CCD camera operated at 200 kV with a point and line resolution of 0.19 nm and 0.14 nm respectively, scaled with Au(100).

Results and discussion

Quantitative Phase Analysis
Pattern matching reveals that only Cu_2O, CuO (tenorite) and Cu are present in all powders in different proportions: quantification done via Rietveld method is proposed in Table 1. As the starting (heat treated) powder is pure Cu_2O (within the limits of detection of XRD), the pres-

ence of the extra phases, and in particular of CuO, has to be attributed to the milling process. In all cases the Rietveld fit is good but not perfect: there is still a certain degree of anisotropic broadening not completely taken into account by our isotropic model, but this should be within the errors presented in Table 1.

Table 1. Quantitative Phase Analysis results obtained from synchrotron data.

Specimen	Milling time (min)	wt% Cu_2O	wt% CuO	wt% Cu
P9-1	1.0	93.5(1)	3.9(1)	2.6(9)
P9-5	5.0	89.4(3)	6.9(5)	3.7(4)
P9-7.5	7.5	90.2(1)	5.1(1)	4.7(2)
P9-10	10.0	92.5(1)	1.7(5)	5.8(8)
P9-20	20.0	88.0(1)	6.0(3)	6.0(4)
P9-40	40.0	86.7(1)	6.5(1)	6.8(3)

It can be seen a clear increase in the content of Cu with the milling time; it cannot be excluded that this phase is actually a mixed Cu/Fe phase. Contamination from the mill is certainly possible and some deposition of a metallic copper film has been observed on the surface of the cup and cylinder. Part of the metallic copper can come from the cuprite - tenorite - copper transformation. Assuming that the transformation occurs in the absence of oxygen, we can see that up to 7wt% Cu could be produced if all present CuO comes from Cu_2O.

Microstructure analysis via WPPM

Synchrotron radiation X-ray diffraction data were analysed by means of the WPPM algorithm assuming the presence of a lognormal distribution of spherical domains. Dislocations were identified as the main cause of strain broadening. Table 2 summarises the main results of the WPPM analysis.

Table 2. WPPM results: unit cell parameter a_0, average domain size <D>, lognormal variance σ, dislocation density ρ, effective outer cut-off radius R_e and Wilkens' parameter $W = Re\ \rho^{1/2}$.

Specimen	Milling Time (min)	a_0 (nm)	<D> (nm)	σ (nm)	ρ (10^{15} m^{-2})	R_e (nm)	Wilkens parameter	GoF
P9-1	1.0	4.2673(1)	45(1)		0.3(2)	11(1)	0.1(1)	2.23
P9-5	5.0	4.2682(6)	20 (1)	67(7)	7(1)	9.0(6)	0.74(1)	1.26
P9-7.5	7.5	4.2709(5)	16(1)	42(13)	21 (1)	5.0(2)	0.72(1)	1.20
P9-10	10.0	4.2744(1)	11.9(9)	21 (3)	30(1)	3.0(1)	0.52(2)	1.24
P9-20	20.0	4.2736(2)	9.3(4)	10 (1)	39(1)	2.3(1)	0.45(2)	1.18
P9-40	40.0	4.2736(2)	9.8(5)	11(1)	42(1)	2.4(1)	0.48(3)	1.10

All specimens but P9-1 gave an excellent fit, as shown e.g. in Figure 1 for the P9-40 specimen. The reason for the poor modelling of P9-1 has to be found in the high grain size inhomogeneity, which in turn is caused by a too short milling time; larger grains (large scattering power) tend to hide the smaller ones (smaller volume, i.e. smaller overall scattering power), thereby leading to incorrect grain statistics evaluation when a wide distribution is present.

As expected, milling causes a reduction in the average size of the coherently diffracting domains and a corresponding increase in the quantity of defects (dislocation density).

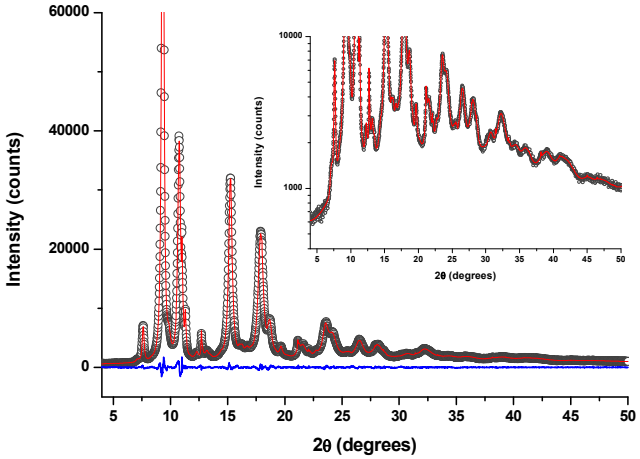

Figure 1. WPPM of the synchrotron X-ray diffraction data for the P9-40 specimen. Data (circle), model (line) and difference between the two (residual, line below). The inset shows the data in log scale to evidence the modelling quality of the tails.

It can be observed a steep variation of those parameters for short milling times, with a levelling (saturation) of the values starting at 20 min effective milling time. It is plausible that the observed phenomenon for shorter milling times corresponds to the formation of dislocation cells [16] as it happens during conventional plastic deformation. The corresponding increase in the cell parameter suggests a pumping of excess volume inside the structure, whereas the levelling after 20 min milling is a clear indicator that a proper nanostructure has been reached. More informative than the mere average size is certainly the size distribution, shown in figure 3 for the whole set of analysed powder.

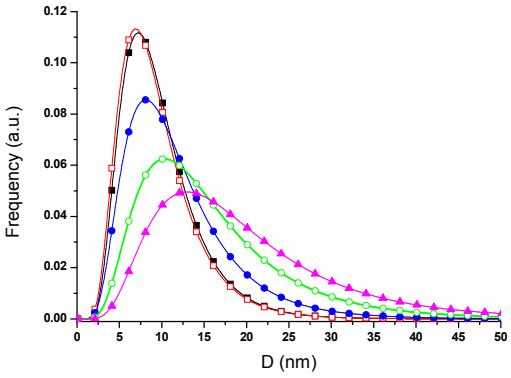

Figure 2. Domain size distribution obtained from WPPM for the specimens analysed in this work. Curves for P9-5 (triangles), P9-7.5 (circles), P9-10 (dots), P9-20 (squares), and P9-40 (diamonds).

It can be observed a progressive narrowing of the distribution, the variation again saturating

at 20 min. It is also interesting to note the trend of Wilkens parameter $W = R_e \rho^{1/2}$, related to the interaction and dipole character of dislocations. The higher the W, the weaker the dipole character and the screening of the displacement field of the dislocations. Lower W values (below unity) indicate enhanced interactions of a high density of dislocations at the grain boundaries leading to nanocrystallinity conditions [17]. In our case, W saturates for P9-20, further validating the hypothesis that after 20 min milling time the nanostructure is reached in the powder.

Scanning and transition electron microscopy

A clear evolution of the powder morphology can be observed by ESEM. The initial powder is characterized by the presence of sharp fragments of various shapes and sizes. After a short milling time (e.g., 1 min) it can be clearly observed the coexistence of fine and coarse particles (figure 3a).

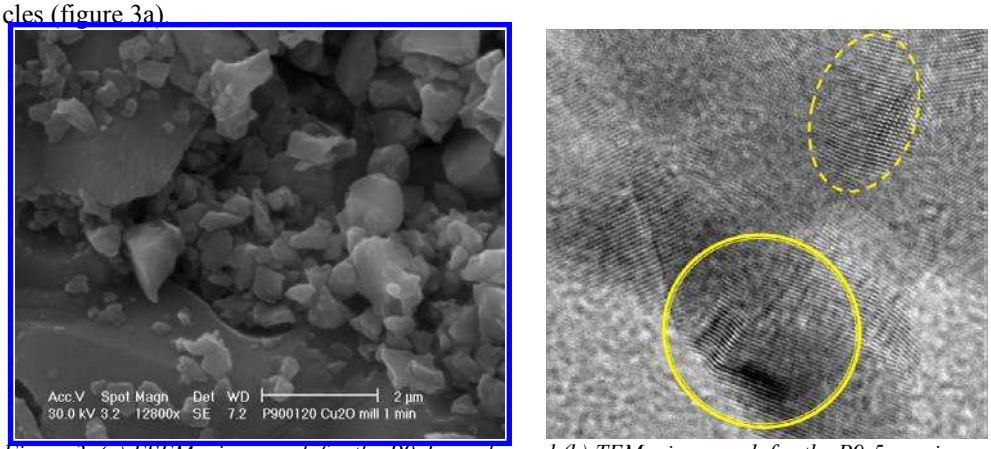

Figure 3. (a) ESEM micrograph for the P9-1 powder and (b) TEM micrograph for the P9-5 specimen.

This can explain the impossibility of getting a proper fit of the XRD data for the P9-1 powder. It is possible that some of the large particles are monocrystalline or composed of a small number of very large domains. Already after 5 minutes of milling, the sharp edges disappear and the small particles start agglomerating over the larger ones. For increasing milling time, a progressive homogenisation of the size and shape of the small particles is observed, with the larger aggregates progressively being formed by large sets of small particles. All morphological observations are compatible with the XRD results. A direct comparison is however not possible, and in any case the observed particle size of the order of 100 nm or more is far larger than the domain size estimated via XRD. This is a clear indication that most of the particles are made of several domains: the milling process contributes to reduce the size of the particles, but also the domain size, with possible introduction of internal grain boundaries. A possible validation for the XRD results comes from the TEM investigation even if the high density of defects and the extensive agglomeration of domains hinders a possible estimation of a size distribution from TEM. HRTEM, on the other hand, allows observing the presence of defects, quantitatively measured by WPPM of the XRD data. Figure 3b shows, for instance, a HRTEM micrograph of the P9-5 specimen: distortion of the lattice planes as well as traces of the presence of dislocations (causing local deformation of the lattice), and possible presence of small angle grain boundary, are evident. All those defects can be caused

by the pileup of a large number of dislocations, and this can justify the large value of the dislocation density observed for this material.
As an Energy Dispersive X-ray Spectroscopy gives unphysical results here (the absolute determination of oxygen in heterogeneous powders like those proposed here is really challenging), it is not possible to identify where CuO and Cu (possibly contaminated by Fe from the milling set) are located.

References

1. Suryanarayana, C., 2001, *Prog. Mater. Sci.*, **46**, 1.
2. Mittemeijer, E.J & Scardi, P. (Editors), 2004, *Diffraction Analysis of the Microstructure of Materials* (Berlin: Springer).
3. Scherrer, P., 1918, Math.-Phys., Kl., 2, 98.
4. Williamson, G.K. & Hall, W.H., 1953, *Acta Metall.,* **1**, 22.
5. Scardi, P. & Leoni, M., 2002, *Acta Crystallogr., Sect. A,* **58**, 190-200.
6. Mittiga, A., Salza, E., Sarto, F., Tucci, M. & Vasanthi, R., 2006, *Appl. Phys. Lett.,* **88**, 163502.
7. Shishiyanu, S.T., Shishiyanu, T.S. & Lupan, O.I., 2006, *Sensors & Actuators B,* **113**, 468.
8. Hara, M., Kondo, T., Komoda, M., Ikeda, S., Shinohara K., Tanaka, A., Kondo, J.N. & Domen, K., 1998, *Chem. Commun.,* 357-358.
9. De Jongh, P.E., Vanmaekelbergh, D. & Kelly, J.J., 1999, *Chem. Commun.,* 1069.
10. Rothenberger, G., Moser, J., Gratzel, M., Serpone, N. & Sharma, D.K., 1985, *J. Am. Chem. Soc.*, **107**, (26), 8054.
11. D'Incau, M., 2008, *High Energy Milling in Nanomaterials Technologies: Process modelling and optimization*, PhD thesis. Università degli Studi di Trento - Italy.
12. Caglioti, G., Paoletti, A. &Ricci, F.P., 1958, *Nucl. Instr. Meth.*, **3**, 223.
13. Leoni, M., Confente, T. & Scardi P., 2006, *Z. Kristallogr. Suppl.*, **23**, 249.
14. Young, R. A., (Editor), 1993, *The Rietveld method,* International Union of Crystallography (Oxford University Press).
15. Bruker AXS. TOPAS Users Manual. 2008 (Karlsruhe, Germany).
16. Xu, Y., Liu, Z. G., Umemoto, M. & Tsuchiya, K., 2002, *Met. Mater. Trans. A*, **33**, 2195.
17. Wilkens, M., 1970, *Phys. Status Solidi (A)*, **2**, 359.

Acknowledgements. Authors wish to acknowledge the European Synchrotron Radiation Facility (ESRF) - Grenoble (France) for the provision of beamtime on the ID31 beamline. Dr A. Fitch is acknowledged for the support on the beamline. Prof. E. Garnier (Univ. Poitiers - France) is acknowledged for the TEM analyses.